Bioorganic Chemistry 107 (2021) 104613

Contents lists available at ScienceDirect

Bioorganic Chemistry

journal homepage: www.elsevier.com/locate/bioorg

Flavonoids from the peels of *Citrus unshiu* Markov. and their inhibitory effects on RANKL-induced osteoclastogenesis through the downregulation of c-Fos signaling *in vitro*

Thi Oanh Vu [a,b], Phuong Thao Tran [c], Wonyoung Seo [c], Jeong Hyung Lee [c], Byung Sun Min [d], Jeong Ah Kim [a,b,*]

[a] College of Pharmacy, Research Institute of Pharmaceutical Sciences, Kyungpook National University, Daegu 41566, Republic of Korea
[b] Vessel-Organ Interaction Research Center, VOICE (MRC), College of Pharmacy, Kyungpook National University, Daegu 41566, Republic of Korea
[c] Department of Biochemistry, College of Natural Sciences, Kangwon National University, Chuncheon, Gangwon-Do 24341, Republic of Korea
[d] College of Pharmacy, Drug Research and Development Center, Daegu Catholic University, Gyeongbuk 38430, Republic of Korea

ARTICLE INFO

Keywords:
Citrus unshiu peels
Flavonols
Flavones
RANKL
Osteoclastogenesis

ABSTRACT

Phytochemical investigation of *Citrus unshiu* peels led to the isolation of eight new flavonols (**7**–**9**, **11**–**15**) and sixteen known compounds (**1**–**6**, **10**, **16**–**24**). Their structures were elucidated using spectroscopic analysis (1D, 2D NMR, and HR-MS). Besides, all isolated compounds (**1**–**24**) were evaluated for their inhibitory effects on receptor activator of RANKL-induced osteoclastogenesis in BMMs. Among them, dimethylmikanin (**1**), quercetogetin (**2**), 3,3′,4′,5,7,8-hexamethoxyflavone (**3**), 3-methoxynobiletin (**4**) showed a significant inhibitory effect on RANKL-induced osteoclast differentiation at a concentration of 10 μM. Moreover, 3-methoxynobiletin (**4**) suppressed RANKL-induced osteoclastogenesis by decreasing the number of osteoclasts and osteoclast actin-ring formation in a dose-dependent manner without causing any cytotoxic effects on BMMs. At the molecular level, 3-methoxynobiletin (**4**) inhibited RANKL-induced c-Fos expression and subsequently NFATc1 activation, as well as the expression of osteoclastogenesis-related marker genes c-Src and CtsK. These findings suggested that 3-methoxynobiletin (**4**) attenuated osteoclast differentiation by inhibiting RANKL-mediated c-Fos signaling and that it may have therapeutic potential for treating or preventing bone resorption-related diseases, such as osteoporosis.

1. Introduction

Osteoporosis is the most common metabolic bone disorder and remains an increasingly significant problem that affects 200 million individuals worldwide [1]. Osteoporosis is characterized by low bone mass and microarchitectural deterioration of bone tissue, leading to enhanced bone fragility and increased fracture risk. An imbalance between osteoclast-mediated bone resorption and osteoblast-induced bone formation is the main cause of the disease [2]. Osteoclasts are large multinucleate cells that differentiate from hematopoietic precursor cells of the monocyte-macrophage lineage following the stimulation of two crucial cytokines, macrophage colony-stimulating factor (M−CSF) and the receptor activator of nuclear factor (NF)-κB ligand (RANKL) [3,4]. The binding of RANKL and its receptor (RANK) triggers numerous downstream signaling events, such as NF-κB and c-Fos signaling, which lead to subsequent activation of the nuclear factor of activated T cells 1 (NFATc1), the master regulator of osteoclastogenesis. The activation of NFATc1 directly regulates the expression of several osteoclastic genes, such as tartrate-resistant acid phosphatase (TRAP), CtsK, and c-Src [5,6].

Citrus unshiu Markov. (Rutaceae), known as Satsuma, Satsuma mandarins, or Satsuma oranges in Western society, are widely cultivated in subtropical countries, such as Korea, Japan, China, and Russia [7]. Their dried fruit peels have been used to improve a variety of digestive dysfunctions, including tympanites, nausea, vomiting, and dyspepsia [8]. The peels have also been traditionally used to improve bronchial and asthmatic conditions as well as cardiac and blood circulation problems in East Asia [9]. Previous chemical and pharmacological studies reported that many actives components, including essential oils, terpenoids, flavonoids, phenolic compounds were isolated from the

* Corresponding author at: College of Pharmacy, Research Institute of Pharmaceutical Sciences, Kyungpook National University, Daegu 41566, Republic of Korea.
E-mail address: jkim6923@knu.ac.kr (J.A. Kim).

https://doi.org/10.1016/j.bioorg.2020.104613
Received 6 November 2020; Received in revised form 18 December 2020; Accepted 28 December 2020
Available online 5 January 2021

peels of *C. unshiu*, and they were indicated to have the antioxidant, anti-carcinogenicity, anti-allergic, anti-diabetic, anti-aging, anti-cancer, and lipid-lowering activities [8]. Therefore, *Citrus* peels have a significant potential to be used as a raw material for cosmetics, pharmaceuticals, and functional foods.

In order to discover more naturally occurring compounds with novel structures and notable bioactive properties for treating or preventing bone resorption-related diseases, such as osteoporosis, phytochemical investigations of the *C. unshiu* peels were undertaken. As a result, 24 compounds were isolated, including eight new flavonols (**7**–**9**, and **11**–**15**). All isolates (**1**–**24**) were further evaluated for their inhibitory effects on RANKL-induced osteoclast formation in bone marrow-derived macrophages (BMMs).

2. Material and methods

2.1. Chemicals, reagents, and antibodies

RANKL was purchased from RandD Systems (Minneapolis, Minnesota, USA), while M−CSF was purchased from Prospec (East Brunswick, New Jersey, USA). Antibodies (anti-c-Fos, anti-Src, anti-α-tubulin, and anti-β-actin) were purchased from Cell Signaling Technology (Beverly, USA). Anti-CtsK antibodies were purchased from Santa Cruz Biotechnology (Santa Cruz, California, USA). Fluorescein Isothiocyanate (FITC)-conjugated phalloidin was obtained from Invitrogen (Carlsbad, California, USA), as were Alexa 488-conjugated anti-rabbit antibodies, and 4′,6-diamidino-2-phenylindole (DAPI). All solvents used for extraction and isolation were of analytical grade and purchased from Duksan Pure Chemicals Co., Ltd. (Kyunggi, South Korea). High-performance liquid chromatography (HPLC) solvents were purchased from Burdick & Jackson (Michigan, USA).

2.2. General experimental procedures

Ultraviolet (UV) spectra were measured with a Thermo 9423AQA2200E UV spectrometer (Thermo Fisher Scientific, Massachusetts, USA). Infrared (IR) spectra were measured with a JASCO FT/IR-4100 spectrometer (Jasco, Tokyo, Japan). High-resolution electrospray ionization mass spectrometry (HR-ESI-MS) spectra were recorded using a Thermo Scientific LTQ Orbitrap XL hybrid four transform mass spectrometer (Thermo Fisher Scientific, Massachusetts, USA). High-resolution fast atom bombardment mass spectrometry (HR-FAB-MS) data were recorded using a JMS-700 model (Jeol, Tokyo, Japan). ^{1}H-(500 MHz), ^{13}C-(125 MHz) NMR, and 2D-NMR spectra were recorded on a Bruker Avance Digital 500 MHz NMR spectrometer (Bruker, Karlsruhe, Germany) (in ppm relative to tetramethylsilane (TMS) as an internal standard, J in Hz at 294 K). Thin-layer chromatography (TLC) was performed using glass plates pre-coated with silica gel 60F_{254} and RP-18 F_{254s} (Merck, Darmstadt, Germany). Compounds were detected under UV light and then visualized by spraying the plates with a 10% sulfuric acid reagent followed by heating to 110 °C for 1 min. Column chromatography (CC) was performed on Merck silica gel (60–200 μm), Merck Lichroprep RP-18 gel (40–63 μm), MCI gel (75–150 μm), and Diaion HP-20 (250–850 μm) (Merck, Darmstadt, Germany). High-performance liquid chromatography (HPLC) was performed with an HPLC Water system (Waters, Middleton, USA) with a 1525 Binary pump, a Water 2998 photodiode array detector, a YMC Pak ODS column (20 × 250 mm, 4 μm), t_R was measured in min.

2.3. Plant material

Citrus unshiu Makov. peels were purchased from a traditional market in Jeonju-si, Korea, in February 2017 and identified by Professor Byung Sun Min at Daegu Catholic University (Daegu, South Korea). A voucher specimen (21A-CU) was deposited at the Laboratory of Pharmacognosy at the College of Pharmacy, Kyungpook National University, South Korea.

2.4. Extraction and isolation

Dried *C. unshiu* peels (10.0 kg) were thoroughly extracted three times with MeOH under reflux at 65 °C for 4 h each. MeOH extract was concentrated in a vacuum to obtain a brown residue (3.3 kg), which was suspended in H_2O and partitioned with solvents to produce five fractions of *n*-hexane (70.5 g), methylene chloride (MC, 105.6 g), ethyl acetate (EtOAc, 66.7 g), *n*-butanol (30.1 g), and a water-soluble layer (2.93 kg).

The MC extract (105.6 g) was subjected to a vacuum liquid chromatography (VLC) silica gel column and eluted with gradient mixtures of *n*-hexane–EtOAc (1:0–1:1, v/v) and MC–MeOH (1:0–0:1, v/v) to yield 12 fractions (1A–1L). Fraction 1I (12.8 g) was chromatographed on a C-18 gel CC using a gradient mixture of MeOH–H_2O (2:1–1:0, v/v) to obtain eight fractions (2A–2I). Fraction 2C (1.85 g) was re-subjected to the MCI gel CC and eluted with an isocratic mixture of MeOH–H_2O (3:1, v/v) to yield five fractions (3A–3E). Fractions 3B (412.4 mg), 3C (603.7 mg), and 3D (135.0 mg) were further purified by a Sephadex LH-20 CC and eluted with MeOH to obtain compounds **19** (24.4 mg), **3** (7.0 mg), **21** (4.0 mg), **1** (2.0 mg) and **17** (3.0 mg), **16** (30.2 mg), **20** (670.8 mg), and **4** (335.9 mg). Compound **18** (187.7 mg) was yielded after recrystallization in MC–MeOH (1:1, v/v) from fraction 3E (314.0 mg). Fraction 2B (6.0 g) was applied to silica gel CC and eluted with a gradient mixture of MC-acetone (9:1–0:1, v/v) to give six fractions (4A–4F). Fraction 4A (703.6 mg) was separated by silica gel CC using an isocratic mixture of MC–acetone (5:1, v/v) to obtain compound **2** (2.0 mg).

The water layer (2.93 kg) was eluted over HP-20 Diaion CC with MeOH-H_2O (0:1–1:0, v/v) to produce four fractions (5A–5D). Fraction 5C (308.6 g) was continuously subjected to VLC with a gradient mixture of MC–MeOH–H_2O (5:1:0.1–7:3:0.5, v/v/v) to yield 12 fractions (6A–6L). Fraction 6C (25.76 g) was applied to silica gel CC and eluted with a gradient mixture of MC–MeOH–H_2O (5:1:0.1–7:3:0.5, v/v/v) to obtain ten fractions (7A–7 J). Fraction 7G (2.1 g) was chromatographed on MCI gel CC with a gradient mixture of MeOH-H_2O (1:1–3:1, v/v) to yield seven fractions (8A–8H). Compounds **7** (4.1 mg) and **8** (2.0 mg) were isolated from fraction 8H (70.5 mg) by using a Sephadex LH-20 CC and eluting with 100% MeOH. Fraction 7I (2.1 g) was separated using MCI gel CC and a gradient mixture of MeOH-H_2O (1:2–1:0, v/v) to produce compound **5** (3.5 mg) and 12 fractions (9A–9L). Fraction 9 K (688.5 mg) was subjected to Sephadex LP-20 CC and eluted with MeOH to yield compounds **13** (80.2 mg), **14** (205.7 mg), and **15** (12.8 mg). Fraction 7H (13.9 g) was subjected to MCI gel CC with a gradient mixture of MeOH–H_2O (1:1–1:0, v/v) to give compound **9** (66.5 mg) and 12 fractions (10A–10 M). Fraction 10E (853.5 mg) was continuously separated by C-18 gel CC and eluted with an isocratic mixture of MeOH–H_2O (2:1, v/v) to obtain compounds **6** (5.0 mg), **12** (25.5 mg), and **11** (6.3 mg). Fraction 6D (7.9 g) was isolated by MCI gel CC with a gradient mixture of MeOH–H_2O (1:1–1:0, v/v) to produce 15 fractions (11A–11O). Fractions 11 K (75.0 mg) and 11*L* (75.5 mg) were further purified by using preparative HPLC and eluting with an isocratic mixture of MeOH–H_2O (40%, 6 ml/min, 60 min) to yield compounds **23** (3.0 mg, t_R = 25.5 min) and **24** (3.0 mg, t_R = 42.0 min). Fractions 6G–6I (230.0 g) were re-chromatographed on VLC silica gels and eluted with a gradient mixture of EtOAc–MeOH–H_2O (9:1:0.2–0:1:0, v/v/v) to obtain five fractions (12A–12E). Fraction 12C (45.3 g) was isolated using silica gel CC and was eluted with an isocratic mixture of EtOAc–MeOH–H_2O (8.5:1.5:0.5, v/v/v) to yield compounds **10** (10.0 mg) and **22** (6.2 mg).

*Citrusunshin A (**7**)*. Yellow powder; UV (λ_{max}, nm, log ε) 256 (4.20), 280 (4.35), 366 (4.17); IR (ν_{max}): 3373, 1714, 1657, 1565, 1448; ^{1}H and ^{13}C NMR: see Table 1; HR-FAB-MS *m/z* 553.1560 $[M]^+$ (calcd 553.1557 for $C_{25}H_{29}O_{14}$).

*Citrusunshin B (**8**)*. Yellow powder; UV (λ_{max}, nm, log ε) 260 (4.18), 275 (4.25), 360 (4.16); IR (ν_{max}): 3357, 1725, 1651, 1565, 1448; ^{1}H and ^{13}C NMR: see Table 1; HR-FAB-MS *m/z* 711.2132 $[M+H]^+$ (calcd 711.2136 for $C_{32}H_{39}O_{18}$).

Table 1
^{1}H (500 MHz) and ^{13}C (125 MHz) NMR spectroscopic data for compounds **7**–**9**, **11**, and **12** (δ in ppm, J in Hz).

Position	**7**[b]		**8**[b]		**9**[a]		**11**[b]		**12**[b]	
	δ_H (J in Hz)	δ_C (mult, J in Hz) dC	δ_H (J in Hz)	δ_C (mult, J in Hz) dC	δ_H (J in Hz)	δ_C (mult, J in Hz) dC	δ_H (J in Hz)	δ_C (mult, J in Hz) dC	δ_H (J in Hz)	δ_C (mult, J in Hz) dC
2		159.1		159.4		153.8		158.0		158.2
3		135.2		135.0		135.5		135.1		134.4
4		180.0		179.8		172.3		179.0		179.0
5		150.0		149.9		143.6		160.0		161.1
6		137.4		137.5		137.5	6.35 d (2.0)	102.0	6.53 s	97.0
7		154.2		154.3		151.0		163.7		159.0
8		134.3		134.3		146.3	6.74 d (2.0)	94.6		125.1
9		146.4		146.3		147.4		148.5		149.2
10		108.3		108.2		114.3		107.5		105.9
1′		122.7		122.3		122.6		122.7		124.8
2′	8.01 d (2.1)	114.2	7.97 d (2.1)	114.1	7.83 d (2.0)	112.3	7.88 d (1.8)	114.4	7.93 d (2.0)	113.9
3′		148.6		148.8		148.1		148.5		148.6
4′		151.7		152.4		151.2		151.6		151.1
5′	6.95 d (8.5)	116.3	6.92 d (8.5)	116.5	7.13 d (8.7)	111.4	6.91 d (8.5)	116.2	6.93 d (8.5)	116.1
6′	7.74 dd (2.1, 8.5)	124.1	7.75 dd (2.1, 8.5)	124.4	7.69 dd (2.0, 8.7)	121.8	7.63 dd (2.0, 8.5)	124.2	7.90 dd (2.0, 8.7)	122.9
1″	5.52 d (7.5)	103.3	5.44 d (7.5)	103.4	5.42 d (7.3)	101.0	5.25 d (7.6)	102.8	5.11 d (7.6)	103.5
2″		76.0		75.6		74.2		74.6[d]		76.4[d]
3″		78.0		75.8		76.3		77.9[e]		77.9[e]
4″		71.6		71.7		70.2		72.4[f]		72.6[f]
5″		78.6		77.9		74.3		75.3[g]		76.0 [g]
6″	3.76 dd (2.2, 12.0) 3.57 dd (5.7, 12.0)	62.6	4.28 dd (2.1, 11.9) 4.10 m[c]	64.5	4.10 d (10.3) 4.22 ddd (1.5, 11.7, 23.3)	63.3	4.30 dd (2.4, 11.6) 3.97 d (8.6)	65.2[h]	4.49 dd (8.3, 10.1)	65.5[h]
1‴				172.1		170.2		171.8[i]		171.4[i]
2‴			2.46 m[c]	45.9	2.36 m[c]	45.1	2.22 d (15.3) 2.14 d (15.3)	47.0	2.24 m[c]	46.5
3‴				70.6		68.8		70.4		70.4
4‴			2.46 m[c]	46.2	2.36 m[c]	45.6	2.40 d (14.2) 2.57 d (14.2)	47.4	2.24 m[c] 2.54 d (13.8)	48.2
5‴				173.0		169.2		172.2[i]		171.9[i]
6‴			1.16 s	27.7	1.02 s	27.1	0.92 s	25.6	0.92 s	27.0
1‴’					5.28 d (8.2)	94.2	5.25 d (7.6)	102.0	5.85 d (7.5)	101.0
2‴’						72.5		75.9[d]		76.3[d]
3‴’						77.9		77.8 [e]		78.2 [e]
4‴’						69.5		72.9[f]		72.1[f]
5‴’						76.4		75.0 [g]		75.4[g]
6‴’						60.1	4.45 m, 4.16 m	65.1 [h]		65.1[h]
5-OCH_3					3.84 s	61.9			3.92 s	57.2
6-OCH_3	3.92 s	61.5	3.92 s	61.5	3.94 s	61.7				
7-OCH_3	4.11 s	62.2	4.12 s	62.3	4.02 s	61.6				
8-OCH_3	3.97 s	62.6	3.98 s	62.6	3.81 s	62.1				
3′-OCH_3	3.98 s	56.7	3.97 s	56.7	3.84 s	55.6	3.94 s	56.7	3.99 s	57.1
4′-OCH_3					3.84 s	55.7				
5‴-OCH_3			3.60 s	51.9						

[a] In DMSO, [b] In CD_3OD, [c] Overlapped, [d-h] Maybe interchangeable.

Citrusunshin C ***(9)***. Yellow powder; UV (λ_{max}, nm, log ε) 258 (4.22), 273 (4.23), 356 (4.16); IR (ν_{max}): 3387, 1722, 1651, 1562, 1430; ^{1}H and ^{13}C NMR: see Table 1; HR-FAB-MS *m/z* 887.2823 $[M+H]^+$ (calcd 887.2821 for $C_{39}H_{51}O_{23}$).

Citrusunshin D ***(11)***. Yellow powder; UV (λ_{max}, nm, log ε) 255 (4.28), 269 (4.35), 358 (4.19); IR (ν_{max}): 3386, 1722, 1651, 1562, 1430; ^{1}H and ^{13}C NMR: see Table 1; HR-ESI-MS *m/z* 807.1990 $[M+Na]^+$ (calcd 807.1960 for $C_{34}H_{40}O_{21}Na$).

Citrusunshin E ***(12)***. Yellow powder; UV (λ_{max}, nm, log ε) 258 (4.23), 273 (4.24), 356 (4.18); IR (ν_{max}): 3377, 1722, 1652, 1562, 1430; ^{1}H and ^{13}C NMR: see Table 1; HR-ESI-MS *m/z* 837.2078 $[M+Na]^+$ (calcd 837.2065 for $C_{35}H_{42}O_{22}Na$).

Citrusunshin F ***(13)***. Yellow powder; UV (λ_{max}, nm, log ε) 254 (4.21), 280 (4.28), 358 (4.16); IR (ν_{max}): 3382, 1722, 1651, 1562, 1430; ^{1}H and ^{13}C NMR: see Table 2; HR-FAB-MS *m/z* 815.2251 $[M+H]^+$ (calcd 815.2246 for $C_{35}H_{43}O_{22}$).

Citrusunshin G ***(14)***. Yellow powder; UV (λ_{max}, nm, log ε) 258 (4.20), 272 (2.25), 358 (4.15); IR (ν_{max}): 3383, 1723, 1651, 1562, 1430; ^{1}H and ^{13}C NMR: see Table 2; HR-FAB-MS *m/z* 845.2355 $[M+H]^+$ (calcd 845.2352 for $C_{36}H_{45}O_{23}$).

Citrusunshin H ***(15)***. Yellow powder; UV (λ_{max}, nm, log ε) 258 (4.23), 275 (4.24), 358 (4.16); IR (ν_{max}): 3387, 1722, 1652, 1562, 1430; ^{1}H and ^{13}C NMR: see Table 2; HR-FAB-MS *m/z* 859.2511 $[M+H]^+$ (calcd 859.2508 for $C_{37}H_{47}O_{23}$).

2.5. Acid hydrolysis

Each compound (1.5 mg) was refluxed in 5 ml of 2 N CF_3COOH for 3 h at 95 °C. After extraction with CH_2Cl_2 (3 × 5 ml), the water layer was dried using an N_2 stream, analyzed using TLC on a silica gel ($CHCl_3$: MeOH: H_2O, 8:5:1), and compared with an authentic sample. Monosaccharide residue was obtained using preparative TLC with the same solvent. The optical rotation of sugar was measured and determined to be D-glucose (positive $[\alpha]_D$) [10].

Table 2
^{1}H (500 MHz) and ^{13}C (125 MHz) for compounds **13**–**15** (δ in ppm, J in Hz) in CD_3OD.

Position	13a		13b		14a		14b		15a		15b	
	δ_H (J in Hz) dC	δ_C (mult, J in Hz) dC	δ_H (J in Hz) dC	δ_C (mult, J in Hz) dC	δ_H (J in Hz) dC	δ_C (mult, J in Hz) dC	δ_H (J in Hz)	δ_C	δ_H (J in Hz) dC	δ_C (mult, J in Hz) dC	δ_H (J in Hz) dC	δ_C (mult, J in Hz) dC
2		158.5		158.5		158.3		158.6		159.1		159.1
3		135.3		135.3		135.0		135.0		135.2		135.2
4		179.4		179.4		179.7		179.7		179.8		179.8
5		150.3		150.3		146.5		146.5		149.8		149.8
6	6.18 s	100.3	6.18 s	100.3		133.0		133.0		137.4		137.4
7		158.9		158.9		152.5		152.5		154.3		154.3
8		129.2		129.2		129.4		129.4		134.3		134.3
9		158.0		158.0		149.5		149.5		146.3		146.3
10		105.6		105.6		105.1		105.1		108.2		108.2
1′		123.0		123.0		123.1		123.1		122.9		122.9
2′	7.97 d (2.0)	114.2	7.97 d (2.0)	114.2	7.97 d (2.0)	114.2	7.97 d (2.0)	114.2	7.96 d (2.0)	114.2	7.96 d (2.0)	114.2
3′		148.4		148.4		148.4		148.4		148.4		148.4
4′		151.0		151.0		151.0		151.0		151.2		151.2
5′	6.94 d (8.5)	116.2	6.94 d (8.5)	116.2	6.95 d (8.5)	116.2	6.95 d (8.5)	116.2	6.93 d (8.5)	116.2	6.93 d (8.5)	116.2
6′	7.74 dd (2.0, 8.5)	124.0	7.74 dd (2.0, 8.5)	124.0	7.74 dd (2.0, 8.5)	124.1	7.74 dd (2.0, 8.5)	124.1	7.72 dd (2.0, 8.5)	124.2	7.72 dd (2.0, 8.5)	124.2
1″	5.36 d (7.3)	103.9	5.36 d (7.3)	104.0	5.35 d (7.3)	103.9	5.35 d (7.3)	103.9	5.40 d (7.3)	103.6	5.40 d (7.3)	103.6
2″	3.00–4.30[c]	75.7[d]	3.00–4.30[c]	75.7[d]	3.17–4.30[c]	75.7 [d]	3.17–4.30[c]	75.7[d]	3.11–4.38[c]	75.6[d]	3.11–4.38[c]	75.6[d]
3″		77.9[e]		77.9 [e]		77.9 [e]		77.9[e]		77.8 [e]		77.9[e]
4″		71.6[f]		71.6[f]		71.6[f]		71.6[f]		71.6[f]		71.6[f]
5″		75.9[g]		75.8[g]		75.8[g]		75.9[g]		75.8[g]		75.9[g]
6″		64.8[h]		64.8[h]		64.8[h]		64.8[h]		64.8[h]		64.8[h]
1‴		172.2		172.2		172.2		172.2		172.2		172.4
2‴	2.52 m[c]	46.0	2.52 m[c]	46.1	2.51 m[c]	46.1	2.51 m[c]	46.1	2.49 m[c]	46.1	2.49 m[c]	46.0
3‴		70.7		70.7		70.7		70.7		70.7		70.7
4‴	2.52 m[c]	46.1	2.52 m[c]	46.1	2.51 m[c]	46.1	2.51 m[c]	46.1	2.49 m[c]	46.1	2.49 m[c]	46.1
5‴		172.5		172.2[i]		172.2[i]		172.2		172.2[i]		172.4
6‴	1.20 s	27.8	1.20 s	27.8	1.20 s	27.8	1.20 s	27.8	1.17 s	27.8	1.17 s	27.8
1⁗	5.11 d (3.6)	94.0	4.52 d (7.8)	98.2	5.11 d (3.6)	94.0	4.52 d (7.8)	98.2	5.11 d (3.6)	94.0	4.51 s (7.8)	98.2
2⁗	3.00–4.30[c]	73.7 [d]	3.00–4.30[c]	76.2[d]	3.17–4.30[c]	73.7 [d]	3.17–4.30[c]	76.2[d]	3.11–4.38[c]	73.7 [d]	3.11–4.38[c]	76.2[d]
3⁗		75.2 [e]		77.8 [e]		75.2 [e]		77.8 [e]		75.2 [e]		77.7 [e]
4⁗		71.9[f]		71.7[f]		71.9[f]		71.6[f]		71.9[f]		71.7[f]
5⁗		70.6[g]		74.7[g]		70.6[g]		74.7[g]		70.6[g]		74.7[g]
6⁗		64.5[h]		64.5[h]		64.5[h]		64.5[h]		64.4[h]		64.4[h]
3′-OCH_3	3.98 s	56.7	3.98 s	56.7	3.98 s	56.7	3.87 s	56.7	3.97, s	56.7	3.97, s	56.7
6-OCH_3					3.92 s	61.2	3.81 s	61.2	3.92, s	61.5	3.92, s	61.5
7-OCH_3									4.11, s	62.3	4.11, s	62.3
8-OCH_3	3.94 s	62.1	3.94 s	62.1	3.96 s	62.1	3.85 s	62.1	3.96, s	62.7	3.96, s	62.7

[c] Overlapped, [d-h] Maybe interchangeable.

2.6. Isolation of BMMs and in vitro osteoclast differentiation assay

Bone marrow cells were isolated from the femurs and tibias of 6-week-old, male mice from the Institute of Cancer Research (DBL, Emseong, Chungbuk, Korea). Each mouse weighed 22–25 g. All mice were housed in a temperature-controlled (24 ± 2 °C) colony room with 55 ± 10% humidity under a 12 h light and dark cycle. All mice were given *ad libitum* access to a standard chow diet and water. Bone marrow cells were cultured in α-Minimal Essential Medium (MEM) (HyClone; GE Healthcare Life Sciences, Logan, UT, USA) containing 10% FBS, 100 U/ml penicillin, 100 μg/ml streptomycin, and 10 ng/ml M−CSF (Prospec-Tany TechnoGene Ltd., East Brunswick, NJ, USA) overnight in a humidified incubator with 5% CO_2 at 37 °C. The floating cells were harvested and maintained for 3 days with 30 ng/ml M−CSF. The cells that adhered to the culture dish were characterized as BMMs and used for subsequent experiments. The BMMs (5×10^4 cells/well) were cultured in 96-well plates and maintained with RANKL (100 ng/ml) and M−CSF (30 ng/ml) for 7 days in the presence or absence of the indicated compounds. The medium was replaced every 2 days. RAW264.7 cells (5×10^4 cells/mL) were seeded onto 96-well plates and incubated with the test compounds in the presence of RANKL (100 ng/mL). The compounds and culture media were replaced every two days for a total of four days. At the end of incubation, cells were fixed for 15 min in 3.7% formalin, permeabilized with 0.1% Triton X-100, and then stained for TRAP with an acid phosphatase leukocyte kit (Sigma-Aldrich; EMD Millipore, Billerica, MA, USA). TRAP-positive multinucleated cells with more than five nuclei were defined as osteoclasts [11].

2.7. Bone resorption and cytotoxicity assays

BMMs (5×10^4 cells/well) were seeded in OsteoAssay Surface 96-well plates (Corning Incorporated, Corning, NY, USA) in α-MEM supplemented with 10% FBS, 1% penicillin and streptomycin, 30 ng/ml M−CSF, 100 ng/ml RANKL, and various concentrations of the positive control (Maslinic Acid (MA)), and compounds **1**–**24**. The culture ran for 7 days, and the medium was replaced every 2 days. The differentiated BMMs were washed with tap water, and images of the resorption pit surfaces were captured using a model H550L microscope (Nikon Corporation, Tokyo, Japan), and quantified via Image J software (Java 1.6.0_20 (64-bit); NIH, Bethesda, MD, USA).

Cytotoxicity was measured using a 3-(4,5-dimethylthiazol-2-yl)-2,5-diphenyl tetrazolium bromide (MTT)-based assay. The BMMs were cultured in 96-well plates (1×104 cells/well) and supplemented with 30 ng/ml M−CSF in the presence of the indicated concentrations of DRG. After 72 h, 0.5 mg/ml of MTT was added to each well for 3 h. At the end of the incubation, the insoluble formazan products were dissolved in dimethyl sulfoxide, and absorbance at 540 nm was determined [11].

2.8. Western blot analysis

Cells were lysed in a lysis buffer [150 mM NaCl, 50 mM Tris-HCl (pH 7.4), 1 mM EDTA, 1% Nonidet P-40, 5 mM sodium orthovanadate, and protease inhibitor cocktail (BD Biosciences, Franklin Lakes, NJ, USA)]. Equal amounts of proteins were separated by SDS-polyacrylamide gel electrophoresis, followed by Western blot analysis. Western blots were incubated overnight with the indicated primary antibodies (1:1,000 dilution), and anti-rabbit or anti-mouse secondary antibodies conjugated to horseradish peroxidase (1: 2,000 dilution) were used to visualize signals using an enhanced chemiluminescence system (ThermoFisher Scientific, Rockford, IL, USA). The band intensity was quantified using Image J software (NIH, Bethesda, MD, USA) [12].

2.9. Immunofluorescence

Cells were rinsed once in phosphate-buffered saline (PBS), fixed in fresh 4% paraformaldehyde for 20 min at room temperature, and permeabilized in 0.5% TritonX-100. Nonspecific sites were blocked using a PBS solution containing 1% goat serum. Cells were then incubated with an anti-NFATc1 (1:200 dilution) antibody. After four washes with PBS, cells were incubated with an Alexa Fluor 488 goat anti-rabbit secondary antibody (1:250 dilution) for 4 h at room temperature, then washed, stained with DAPI, and mounted. Confocal images were acquired using an OLYMPUS FV1000 inverted laser scanning confocal microscope equipped with an external argon laser, HeNe laser Green, and HeNe laser Red. Images were captured at the colony midsection using a UPLSAPO 60X NA1.35 oil immersion objective (OLYMPUS) [12].

2.10. Statistical analysis

All experimental data are presented as the mean ± standard error of the mean from at least three independent experiments. Statistical significance was assessed by one-way analysis of variance and Tukey's posthoc corrections for multiple comparisons to examine differences between the two groups using SPSS version 14.0 (SPSS Inc., Chicago, IL, USA). P values < 0.05 were considered statistically significant.

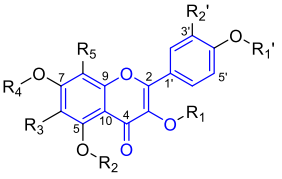

	R_1	R_2	R_3	R_4	R_5	R_1'	R_2'	R''
1	CH_3	CH_3	OCH_3	CH_3	H	CH_3	H	-
2	CH_3	CH_3	OCH_3	CH_3	H	CH_3	OCH_3	-
3	CH_3	CH_3	H	CH_3	OCH_3	CH_3	OCH_3	-
4	CH_3	CH_3	OCH_3	CH_3	OCH_3	CH_3	OCH_3	-
5	Rut	H	H	H	H	H	OH	-
6	H	H	H	Rut	H	H	OCH_3	-
7	1-Glc	H	OCH_3	CH_3	OCH_3	H	OCH_3	-
8	A	H	OCH_3	CH_3	OCH_3	H	OCH_3	OCH_3
9	A	CH_3	OCH_3	CH_3	OCH_3	CH_3	OCH_3	1-OGlc
10	A	H	H	H	OCH_3	H	OCH_3	OH
11	H	H	H	A	H	H	OCH_3	6-Glc(β)
12	H	CH_3	H	H	OA	H	OCH_3	6-Glc(β)
13	A	H	H	H	OCH_3	H	OCH_3	6-Glc
14	A	CH_3	H	H	OCH_3	H	OCH_3	6-Glc
15	A	CH_3	OCH_3	H	OCH_3	H	OCH_3	6-Glc

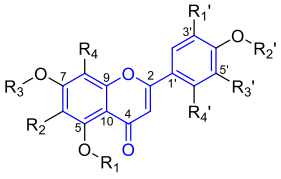

	R_1	R_2	R_3	R_4	R_1'	R_2'	R_3'	R_4'
16	CH_3	H	CH_3	OCH_3	CH_3	H	H	H
17	CH_3	OCH_3	CH_3	H	CH_3	H	H	H
18	CH_3	OCH_3	CH_3	OCH_3	CH_3	H	H	H
19	CH_3	H	CH_3	OCH_3	CH_3	OCH_3	H	H
20	CH_3	OCH_3	CH_3	OCH_3	CH_3	OCH_3	H	H
21	CH_3	H	CH_3	OCH_3	CH_3	OCH_3	OCH_3	OCH_3
22	H	H	H	Xyl	H	H	H	H
23	H	H	H	1-Glc	CH_3	OH	H	H
24	H	1-Glc	H	H	CH_3	OH	H	H

1-Glc **6-Glc**

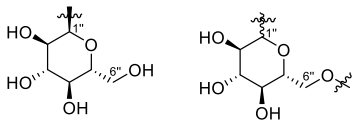

A **Rut** **Xyl**

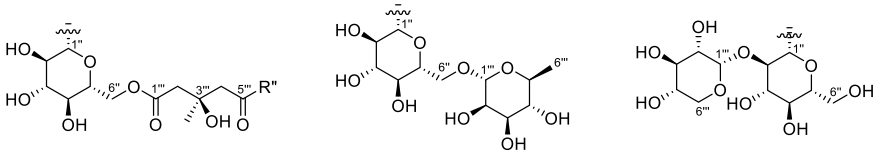

Fig. 1. Chemical structures of isolated compounds from *C. unshiu* peels.

3. Results and discussions

3.1. Structural determination of compounds 1–24

Using repeated CC (silica gel, MCI, Sephadex LH-20, preparative HPLC), 24 compounds, including eight new compounds (**7**–**9**, **11**–**15**), were isolated from the *C. unshiu* peels (Fig. 1). The chemical structures of the known compounds were identified by comparison of their spectroscopic data with those reported previously in the literature, and included: dimethylmikanin (**1**) [13], quercetogetin (3,3′,4′,5,6,7-hexamethoxyflavone) (**2**) [14], 3,3′,4′,5,7,8-hexamethoxyflavone (**3**) [15], 3-methoxynobiletin (3,5,6,7,8,3′,4′-heptamethoxyflavone) (**4**) [15], rutin (**5**) [16], isorhamnetin 7-*O*-rutinoside (**6**) [17], limocitrunshin (**10**) [18], 6-demethoxytangeretin (**16**) [19], 5,6,7,4′-tetramethoxyflavone (**17**) [20], tangeretin (**18**) [19], 6-demethoxynobiletin (3′,4′,5,7,8-pentamethoxyflavone) (**19**) [19], nobiletin (**20**) [19], 5,7,8,2′,3′,4′,5′-heptamethoxyflavone (**21**) [21], vitexin 2″-*O*-xyloside (**22**) [22], diosmetin 8-*C*-glucoside (**23**) [23], and diosmetin 6-*C*-glucoside (**24**) [23]. The structure elucidation of the new compounds (**7**–**9**, **11**–**15**) was established according to their derivatives (**1**–**6** and **10**) together with the 1D, 2D NMR and HR-MS spectra.

Compound **7** was isolated as a yellow powder, and its molecular formula was determined as $C_{25}H_{28}O_{14}$ by the HR-FAB-MS ion at *m/z* 553.1560 $[M+H]^+$ (calcd for $C_{25}H_{29}O_{14}$, 553.1557) (Fig. S1.9, Supporting Information). UV absorption bands at 256, 280, and 366 nm suggested that compound **7** is a flavonol derivative. Its IR spectrum indicated the presence of hydroxyl (3373 cm^{-1}), carbonyl (1714 cm^{-1}), conjugated carbonyl (1657 cm^{-1}), and aromatic (1565, 1448 cm^{-1}) groups. The ^1H NMR spectrum of **7** displayed signals of an ABM coupling system at δ_H 8.01 (1H, d, $J = 2.1$ Hz), 7.74 (1H, dt, $J = 2.1$, 8.5 Hz), and 6.95 (d, 1H, $J = 8.5$ Hz). Additionally, the ^1H NMR spectrum also exhibited four methoxy protons at δ_H 3.92 (6-OCH_3), 3.97 (8-OCH_3), 3.98 (3′-OCH_3), and 4.11 (7-OCH_3) (Table 1). In the ^{13}C NMR spectrum, the characteristic signals of a flavone skeleton at δ_C 159.1 (C-2), 135.2 (C-3), 180.0 (C-4), 150.0 (C-5), 137.4 (C-6), 154.2 (C-7), 134.3 (C-8), 146.4 (C-9), 108.3 (C-10), 122.7 (C-1′), 114.2 (C-2′), 148.6 (C-3′), 151.7 (C-4′), 116.3 (C-5′), and 124.1 (C-6′) and four methoxy groups at δ_C 61.5 (6-OCH_3), 62.2 (7-OCH_3), 62.6 (8-OCH_3), and 56.7 (3′-OCH_3) were observed (Table 1). The location of methoxy groups at C-6, C-7, C-8, and C-3′ was confirmed by the heteronuclear multiple bond correlations (HMBCs) between δ_H 3.92 and δ_C 137.4 (C-6), between δ_H 3.97 and δ_C 134.3 (C-8), between δ_H 3.98 and δ_C 148.6 (C-3′), and between δ_H 4.11 and δ_C 154.2 (C-7), respectively (Fig. 2). In addition, a glucopyranosyl moiety was assumed from the signals between δ_H 3.28 and 5.52 in the ^1H NMR spectrum together with a set of characteristic signals at δ_C 103.3 (C-1″), 78.6 (C-5″), 78.0 (C-3″), 76.0 (C-2″), and 62.6 (C-6″) in the ^{13}C NMR spectrum (Table 1). Furthermore, *β*-form of glucopyranosyl moiety was deduced by the large coupling constant $J = 7.5$ Hz of anomeric proton [24]. After acid hydrolysis, the sugar unit was determined to be D-glucose, which was identified by comparison of TLC data and optical rotation $[\alpha]_D^{21.0}$ + 50.8 (c 0.2, H_2O) with those of authentic samples [10,25,26]. The location of a glucopyranosyl moiety at C-3 of aglycone was confirmed by the HMBC between H-1″ and C-3 (Fig. 2). Thus, compound **7** was identified as 5,4′-dihydroxy-6,7,8,3′-tetramethoxyflavone 3-*O*-*β*-D-glucoside and named citrusunshin A.

Compound **8** was a yellow powder and was assigned the molecular formula $C_{32}H_{38}O_{18}$ from its HR-FAB-MS ion at *m/z* 711.2132 $[M+H]^+$ (calcd for $C_{32}H_{39}O_{18}$, 711.2136) (Fig. S1.18, Supporting Information). Its IR spectrum showed an absorption band for hydroxyl (3357 cm^{-1}), carbonyl (1725 cm^{-1}), conjugated carbonyl (1651 cm^{-1}), and aromatic (1565, 1448 cm^{-1}) groups. The ^1H and ^{13}C NMR data of compound **8** were similar to those of compound **7**, except for the additional signals of two carbonyl groups at δ_C 172.1 (C-1‴), 173.0 (C-5‴); an oxygenated quaternary carbon at δ_C 70.6 (C-6‴); two methylene groups at δ_H 2.46 (4H, m) and δ_C 45.9 (C-2‴), 46.2 (C-4‴); a *tert*-methyl at δ_H 1.16 (3H, s) and δ_C 27.7 (C-6‴) which were determined to be a 3-hydroxy-3-methylglutaroyl (HMG) moiety (Tables 1). Further confirmation was deduced

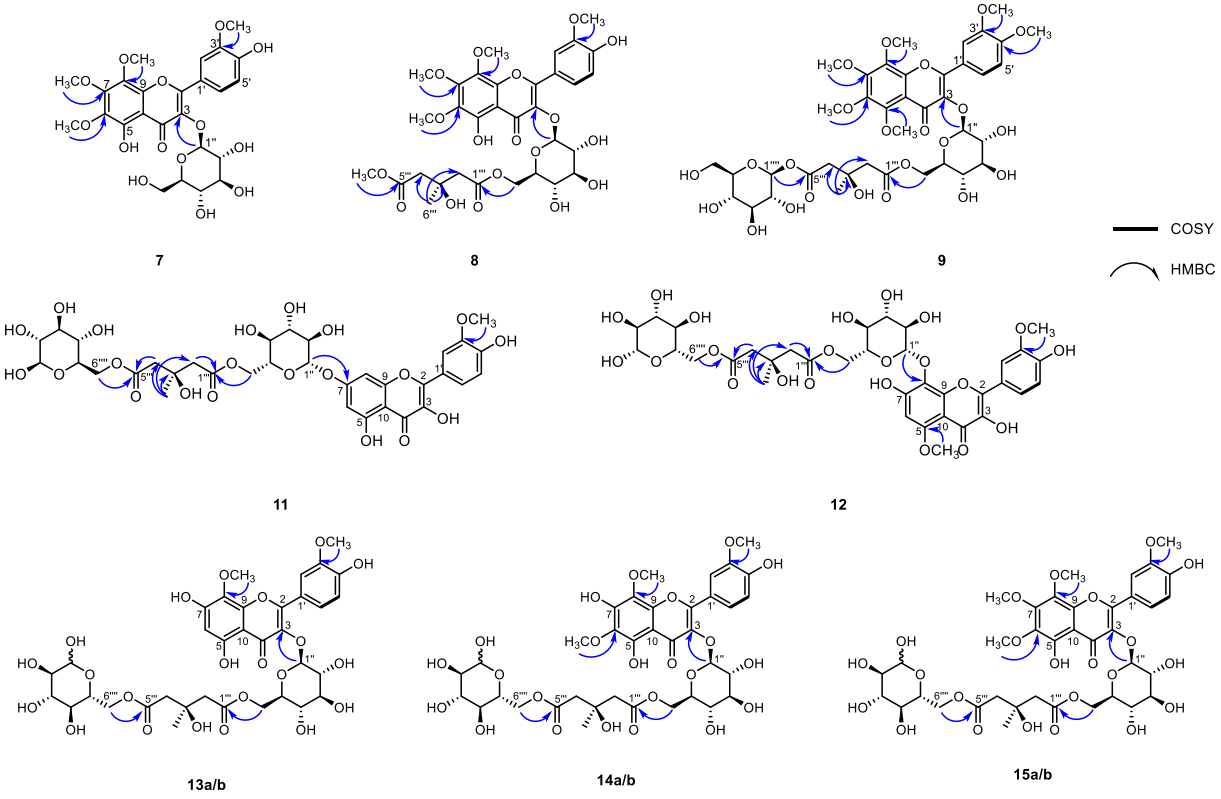

Fig. 2. Key ^1H–^1H COSY and HMBC correlations of **7–9** and **11–15.**

by HMBCs from H-2‴ to C-1‴, C-3‴, C-4‴, and C-6‴, from H-4‴ to C-2‴, C-3‴, C-5‴, and C-6‴, from H-6‴ to C-2‴, C-3‴, and C-4‴ (Fig. 2). In addition, an upfield methoxy group at δ_H 3.60 (3H, s) and δ_C 51.9 (5‴–OCH_3) was also observed in the ^{1}H and ^{13}C NMR spectra of **8**. The location of this methoxy at C-5‴ was confirmed by an HMBC from 5‴–OCH_3 to C-5‴. The downfield chemical shift of C-6″ (δ_C 64.5) in **8** compared to the C-6″ of glucose in **7** (δ_C 62.6) suggests that the HMG moiety is at position C-6″. This was also confirmed by an HMBC from H-6″ to C-1‴ (Fig. 2). The *S*-configuration for C-3‴ of HMG was determined as a natural product since naturally occurring HMG esters formed *via* the acylation of the hydroxyl group with (*S*)-HMG-CoA possess an (*S*)-configuration at the C-3 stereogenic carbon [27,28]. These data led us to conclude that the structure of compound **8** was 5,4′-dihydroxy-6,7,8,3′-tetramethoxyflavone 3-*O*-[(3*S*)-3-hydroxy-3-methyl-methylglutaroyl (1 → 6)]-*β*-D-glucoside and named citrusunshin B.

Compound **9** was isolated as a yellow powder. Its molecular formula was established as $C_{39}H_{50}O_{23}$ by the HR-FAB-MS ion at *m/z* 887.2823 $[M+H]^+$ (calcd for $C_{39}H_{51}O_{23}$, 887.2821) (Fig. S1.27, Supporting Information). Its IR spectrum showed absorption bands at 3386, 1722, 1651, 1562, and 1430, which suggested that hydroxy, carbonyl, and aromatic groups were present. The ^{1}H NMR and ^{13}C NMR spectra exhibited a flavonol skeleton, two sugar units, an HMG moiety, and six methoxy groups (Table 1). The 1D NMR data of compound **9** were similar to those of compound **8** except for the replacement of a methoxy group at the C-5‴ (δ_C 51.9) of HMG moiety by a glucose unit (δ_H 5.28, δ_C 94.2, 72.5, 77.9, 69.5, 76.4, 60.1) in compound **9** (Fig. 2). This was also confirmed by the HMBC of the anomeric proton H-1‴’ (δ_H 5.28) with C-5‴ (171.4) (Fig. 2). Acid hydrolysis of compound **9** produced D-glucose using TLC ($CHCl_3$–MeOH–H_2O = 8:5:1, R_f 0.30) and optical rotation $[\alpha]_D^{21.0}$ +50.8 (c 0.2, H_2O) in comparison with those of authentic samples [10,25,26]. The orientation of the glucopyranosyl moieties was deduced to be *β*, according to the large coupling constant of the anomeric protons at δ_H 5.42 (1H, d, J = 7.3 Hz) and 5.28 (1H, d, J = 8.2 Hz). Furthermore, a comparison of the NMR data of compounds **8** and **9** also indicated the presence of two extra methoxy groups δ_H 3.84 (6H, 5-OCH_3, 4′-OCH_3) at C-5 and C-4′ in **9**. The HMBC correlations between these methoxy groups and C-5 and C-4′ further confirmed their locations (Fig. 2). Thus, compound **9** was defined as 5,6,7,8,3′,4′-hexamethoxy-flavonone-3-*O*-[*β*-D-glucopyranosyl(6 → 5)-3(*S*)-3-hydroxy-3-methylglutarate-(1 → 6)]-*β*-D-glucopyranoside and named citrusunshin C.

Compound **11** was obtained as a yellow powder. Its molecular formula was determined as $C_{34}H_{40}O_{21}$ by the HR-ESI-MS ion at *m/z* 807.1990 $[M+Na]^+$ (calcd for $C_{34}H_{40}O_{21}Na$, 807.1960) (Fig. S1.36, Supporting information). Its IR spectrum suggested the presence of hydroxy (3386 cm^{-1}), carbonyl (1722, 1651 cm^{-1}), and aromatic (1562, 1430 cm^{-1}) groups. The ^{1}H NMR spectrum showed signals for five aromatic protons corresponding to the meta coupled protons δ_H 6.35 (1H, d, J = 2.0 Hz, H-6) and 6.74 (1H, d, J = 2.0 Hz, H-8) on the A ring and the ABM coupling system δ_H 7.88 (1H, d, J = 1.8 Hz, H-2′), 7.63 (1H, dd, J = 1.8, 8.5 Hz, H-6′), and 6.91 (1H, d, J = 8.5 Hz, H-5′) on the B ring of the flavonoid. A methoxy group at δ_H 3.94 (3H, s, 3′-OCH_3) was also observed (Table 1). The ^{13}C spectrum revealed signals for 34 carbons, of which 16 signals were ascribed to isorhamnetin, including a carbonyl group (δ_C 179.0, C-4) and methoxy group (δ_C 56.7, 3′-OCH_3). The remaining signals were attributed to two glucopyranosyl units and an HMG moiety, which were verified by HMBCs. After acid hydrolysis, the sugar units were confirmed to be D-glucose by the same method used for compounds **8** and **9**. The *β*-configuration for the two sugar moieties was also determined based on the large coupling constant (J = 7.6 Hz) of anomeric protons at δ_H 5.25 (2H, H-1″, H-1‴’). The position of one of the *β*-D-glucopyranosyl moieties at C-7 was confirmed by the HMBC between H-1″ (δ_H 5.25) and C-7 (δ_C 163.7). The HMBC of H-6″ (δ_H 4.30 and 3.97) with C-1‴ (δ_C 171.8) and between H-6‴’ (δ_H 4.45 and 4.16) and C-5‴ (δ_C 172.2) suggested that these glucose units were connected *via* an HMG moiety (Fig. S1.34, Supporting Information). Based on the above data analyses, compound **11** was determined to be isorhamnetin-7-*O*-[*β*-D-glucopyranosyl-(6 → 5)-(3*S*)-3-hydroxy-3-methylglutarate(1 → 6)]-*β*-D-glucopyranoside and named citrusunshin D.

Compound **12** was isolated as a yellow powder. Its HR-ESI-MS spectrum exhibited an ion at *m/z* 837.2078 $[M+Na]^+$ (calcd 837.2065 for $C_{35}H_{42}O_{22}Na$), which consistent with a molecular formula of $C_{35}H_{42}O_{22}$ (Fig. S1.45, Supporting Information). The ^{1}H, ^{13}C NMR, and distortionless enhancement by polarization transfer spectra (DEPT) of compound **12** revealed signals of a flavone aglycone, two *β*-glucopyranosyl units, and an HMG moiety (Table 1). The ^{1}H and ^{13}C NMR data of compound **12** were almost identical to those of compound **11**, except for the addition of a methoxy group at C-5 and the absence of a singlet proton H-8. In addition, the HMBC spectrum indicated a linkage between H-1″ (δ_H 5.11) and C-8 (δ_H 125.1), which suggested that the position of this *β*-glucopyranosyl unit (δ_H 5.11) was located at C-8, instead of at C-7 in compound **11** (Fig. 2). Furthermore, the HMBCs between methoxy groups δ_H 3.92 (5-OCH_3) and 3.99 (3′-OCH_3) with C-5 and C-3′ confirmed the location of these groups. The connection of two glucose moieties *via* an HMG moiety was also determined by the HMBC cross-peaks of H-6″/C-1‴ and H-6‴’/C-5‴ (Fig. 2). The positions of the remaining functional groups were based on the HMQC and HMBC spectra (Figs. S1.43 and S1.44, Supporting Information). Therefore, compound **12** was elucidated to be 3,7,4′-trihydroxy-5,3′-dimethyl-flavone-8-*O*-[*β*-D-glucopyranosyl-(6 → 5)-(3*S*)-3-hydroxy-3-methyl-glutarate-(1 → 6)-*β*-D-glucopyranoside and named citrusunshin E.

Compound **13** was isolated as a yellow powder and observed in the ^{1}H and ^{13}C NMR spectra as a mixture of anomeric forms (**13a**, **13b**), with a ratio of ~1:1. The molecular formulas of **13a** and **13b** were established as $C_{35}H_{42}O_{22}$ by the HR-FAB-MS ion at *m/z* 815.2251 $[M+H]^+$ (calcd for $C_{35}H_{43}O_{22}$, 815.2246) (Fig. S1.54, Supporting Information). The ^{1}H NMR spectrum of compounds **13a** and **13b** was similar to those of the co-isolated limocitrunshin (**10**), except for the addition of two anomeric protons δ_H 5.11 (1H, d, J = 3.6 Hz) and 4.52 (1H, d, J = 7.8 Hz) (Table 2). These anomers were determined to be *α*- and *β*-D-glucopyranosyl based on their coupling values (**13a**: J = 3.6 Hz and **13b**: J = 7.8 Hz). In both cases, the locations of additional *α*- and *β*-D-glucopyranosyl were identified at C-5‴ of limocitrunshin by the HMBC between H-6‴’ and C-5‴ (Fig. 2) as well as the evidence of the downfield shift of C-6‴ to δ_C 64.4 (Table 2). Therefore, the structure of compound **13** was determined to be limocitrunshin-6-*O*-glucopyranoside and named citrusunshin F.

Compound **14** was isolated as a yellow powder. Its molecular formula was established as $C_{36}H_{44}O_{22}$ by the HR-FAB-MS ion at *m/z* 845.2355 $[M+H]^+$ (calcd for $C_{36}H_{45}O_{22}$, 845.2352) (Fig. S1.63, Supporting Information). Compound **14** was also determined to be a mixture of *α*- and *β*-anomers of glucose (Table 2). The ^{1}H NMR spectrum of compound **14** was very similar to that of compound **13**, except for an extra methoxy group at δ_H 3.92. The position of this methoxy at C-6 was confirmed by the HMBC from 6-OCH_3 (δ_H 3.92) to C-6 (δ_C 133.0) (Fig. 2). Thus, the structure of compound **14** was elucidated as 6-methoxy-limocitrunshin (5 → 6)-*O*-glucopyranoside and named citrusunshin G.

Compound **15** was isolated as a yellow powder. Its molecular formula was established as $C_{37}H_{46}O_{23}$ by the HR-FAB-MS ion at *m/z* 859.2511 $[M+H]^+$ (calcd for $C_{37}H_{47}O_{23}$, 859.2508) (Fig. S1.72, Supporting Information). The 1D NMR spectra of compound **15** also displayed the presence of both the *α*- and *β*- glucose anomers. (Table 2). The ^{1}H NMR spectrum of compound **15** was very similar to that of compound **14** except for an extra a methoxy group at δ_H 4.11. The position of this methoxy at C-7 was confirmed by the HMBC from 7-OCH_3 (δ_H 4.11) to C-7 (δ_C 154.3) (Fig. 2). Thus, the structure of **15** was elucidated as 4-dehydroxy-6,7-dimethoxy-limocitrunshin (5 → 6)-*O*-glucopyranoside and named citrusunshin H.

3.2. Anti-osteoclastogenic effect assay

To evaluate the anti-osteoclastogenic effect of the isolated compounds **1**–**24**, we used two standard osteoclast differentiation *in vitro* models, RAW264.7 cells model and BMMs model. For primary screening, RAW264.7 cells were stimulated with RANKL in the presence of 10 μM of compounds **1**–**24**. Among them, four compounds, including dimethylmikanin (**1**), quercetogetin (3,3′,4′,5,6,7-hexamethoxyflavone) (**2**), 3,3′,4′,5,7,8-hexamethoxyflavone (**3**), 3-methoxynobiletin (3,5,6,7,8,3′,4′-heptamethoxyflavone) (**4**), inhibited RANKL-induced formation of TRAP-positive multinucleated osteoclasts (Fig. S3.2, Supporting Information). To further confirm the anti-osteoclastogenic effects of compounds **1**–**4**, we employed BMMs model. BMMs were stimulated with M−CSF and RANKL in the presence of various concentrations of compounds **1**–**4**. The number of osteoclasts decreased in the presence of compounds **1**–**4** (Fig. 3A and B). Maslinic acid was used as a positive control [29]. Maslinic acid also inhibited RANKL-induced osteoclastogenesis with the IC_{50} value of 1.2 ± 0.6 μM (Fig. S3.2, Supporting Information). Next, the effect of these compounds (**1**–**4**) on cell viability of BMMs was determined. None of the active compounds significantly decreased cell viability of BMMs, even at a concentration of 30 μM. Instead, compound **3** considerably increased the cell viability of BMMs at concentrations used in this study, suggesting that the anti-osteoclastogenic activity of compounds (**1**–**4**) was not mediated by decreasing cell viability of BMMs (Fig. 3**C**).

Next, we compared the anti-osteoclastogenic effects of these compounds (**1**–**4**) in BMMs. Among them, compound **4** showed the most potent inhibitory effect on RANKL-induced TRAP-positive

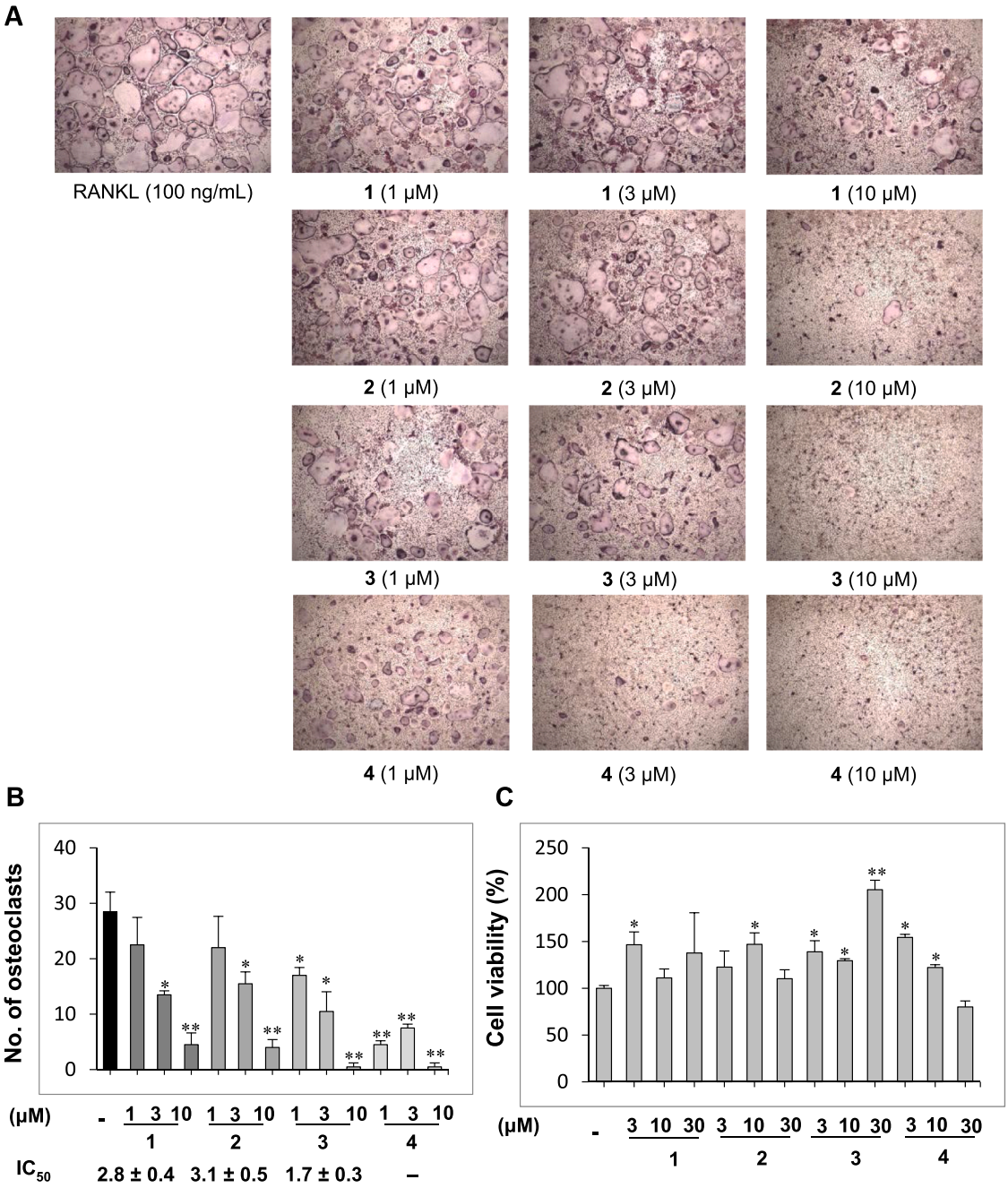

Fig. 3. Effects of active flavonols on RANKL-induced osteoclastogenesis in BMMs (A and B). Flavonols inhibit RANKL-induced differentiation of BMMs into osteoclasts. (C) Cell viability was measured by the MTT assay. Data are presented as the mean ± SE (*P < 0.05, **P < 0.01, versus vehicle-treated control; n = 3).

multinucleated osteoclasts. Thus, compound **4** was subsequently tested for the dose-dependent inhibition of RANKL-induced osteoclast formation. As shown in Fig. 4A and B, compound **4** exhibited inhibitory effects in a dose-dependent manner. Therefore, we further investigated the effects of compound **4** in more detail.

By examining whether compound **4** could inhibit actin-ring formation, an essential characteristic of mature osteoclasts. Stimulation of BMMs with RANKL and M−CSF resulted in the formation of an actin-ring structure, as evidenced by FTTC-phalloidin staining, however, the size and density of the actin-ring structure significantly decreased in a concentration-dependent manner in the presence of compound **4** (Fig. 4**D**). These results indicate that compound **4** suppressed RANKL-induced formation of mature osteoclasts.

To evaluate whether the inhibition of osteoclast differentiation and formation by compound **4** was caused by its potential cytotoxic effects, an MTT assay was conducted. Compound **4** did not exhibit cytotoxicity in BMMs at a concentration of up to 30 μM (Fig. 4**C**). To determine the inhibitory effect of compound **4** during the early or late stages of osteoclastogenesis, we tested the effects of compound **4** on RANKL-induced osteoclast precursor differentiation by treating RANKL-stimulated BMMs with compound **4** at different times from day 0 to day 3. Compound **4** extremely inhibited RANKL-induced osteoclast differentiation on day 1 but did not effectively inhibit osteoclast differentiation on day 3 (Fig. 4**E**), which suggests that compound **4** inhibits RANKL-induced osteoclast differentiation during an early stage of differentiation.

In osteoclast precursors, c-Fos is known to play an important role during the early stage of osteoclast differentiation *via* a RANKL-mediated pathway [30]. To investigate the mechanisms by which compound **4** suppressed RANKL-induced osteoclast formation, the

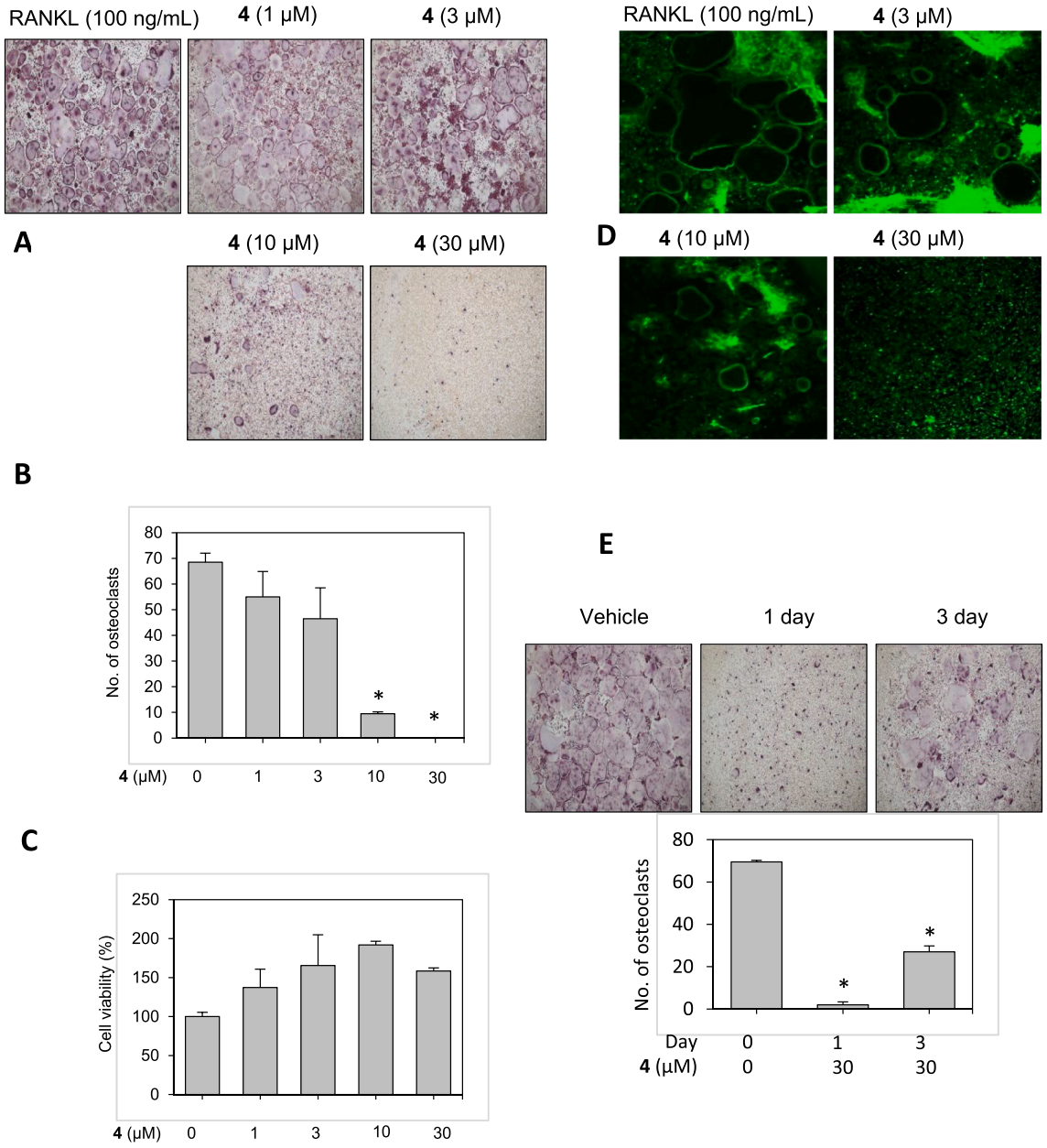

Fig. 4. Compound **4** inhibits RANKL-induced osteoclastogenesis in BMMs. (A and B) Compound **4** inhibits RANKL-induced differentiation of BMMs into osteoclasts in a dose-dependent manner. (C) Cell viability was measured using the MTT assay. (D) Compound **4** suppresses RANKL-induced actin-ring formation. (E) Compound **4** inhibits RANKL-induced osteoclast formation during an early stage of differentiation. Data are presented as the mean ± SE (*P < 0.01, versus vehicle-treated control; n = 3).

inhibitory effect of **4** on RANKL-induced c-Fos expression was examined. While BMMs were stimulated, which led to an increase in the expression of c-Fos, RANKL-induced c-Fos expression was significantly decreased in a dose-dependent manner (Fig. 5**A**), indicating that compound **4** suppressed RANKL-induced osteoclastogenesis *via* modulation of the c-Fos signaling pathway.

NFATc1 is a master transcription factor of osteoclast formation following RANKL stimulation. The enhanced expression of NFATc1 was associated with an efficient induction of mature osteoclasts [31]. A previous study demonstrated that c-Fos signaling is important for the activity of the osteoclast differentiation transcription factor NFATc1. Since compound **4** suppressed RANKL-induced c-Fos expression, we designed an assay to evaluate the effect of compound **4** on RANKL-induced NFATc1 expression. As shown in Fig. 5**B**, the expression level of NFATc1 decreased dose-dependently. We next determined the effects of compound **4** on the expression of osteoclastogenesis-related target genes, such as CtsK and c-Src, which are downstream genes of the NFATc1 pathway. The expression level of these genes was attenuated during RANKL-induced osteoclastogenesis (Fig. 5**C**). These results demonstrate that compound **4** suppressed RANKL-induced NFATc1 activation by decreasing c-Fos signaling.

3.3. The structure–activity relationship (SAR) analysis

In this study, the SAR analysis was valuable guidance to identify and understand new bioactive components from *C. unshiu* peels. 24 isolated compounds, including fifteen flavonols (**1**–**15**) and nine flavones (**16**–**24**), were evaluated for their anti-osteoclastogenesis effects (Fig. S3.2, Supporting information). We realized that flavonols inhibited RANKL-induced osteoclast formation without causing cytotoxicity, whereas flavones did not show any inhibitory effects at the concentrations used in this study. We also found that the OCH_3 group at the C-3 of flavonols played an indispensable role in the inhibition of osteoclast formation (Figs. 1 and 3). When the OCH_3 group at C-3 was replaced by other groups, such as OH, glucopyranosyl, or derivatives of glycopyranosyl, compounds **5**–**15** did not show any inhibitory effects, whereas compounds **1**–**4** containing an OCH_3 group at C-3 significantly inhibited RANKL-induced osteoclastogenesis. The importance of the OCH_3 group at the C-3 of flavonoids was further confirmed by comparison of the inhibitory effects of multimethoxy flavones (**16**–**21**) and multimethoxy flavonols (**1**–**4**). The absence of an OCH_3 group at C-3 in compounds **16**–**21** resulted in no inhibition of RANKL-induced osteoclast differentiation. In addition, among four active flavonols (**1**–**4**), the main outcomes show that the number of OCH_3 and the position of OCH_3 groups at C-8 are crucial. For example, compound **4** contained seven OCH_3 groups

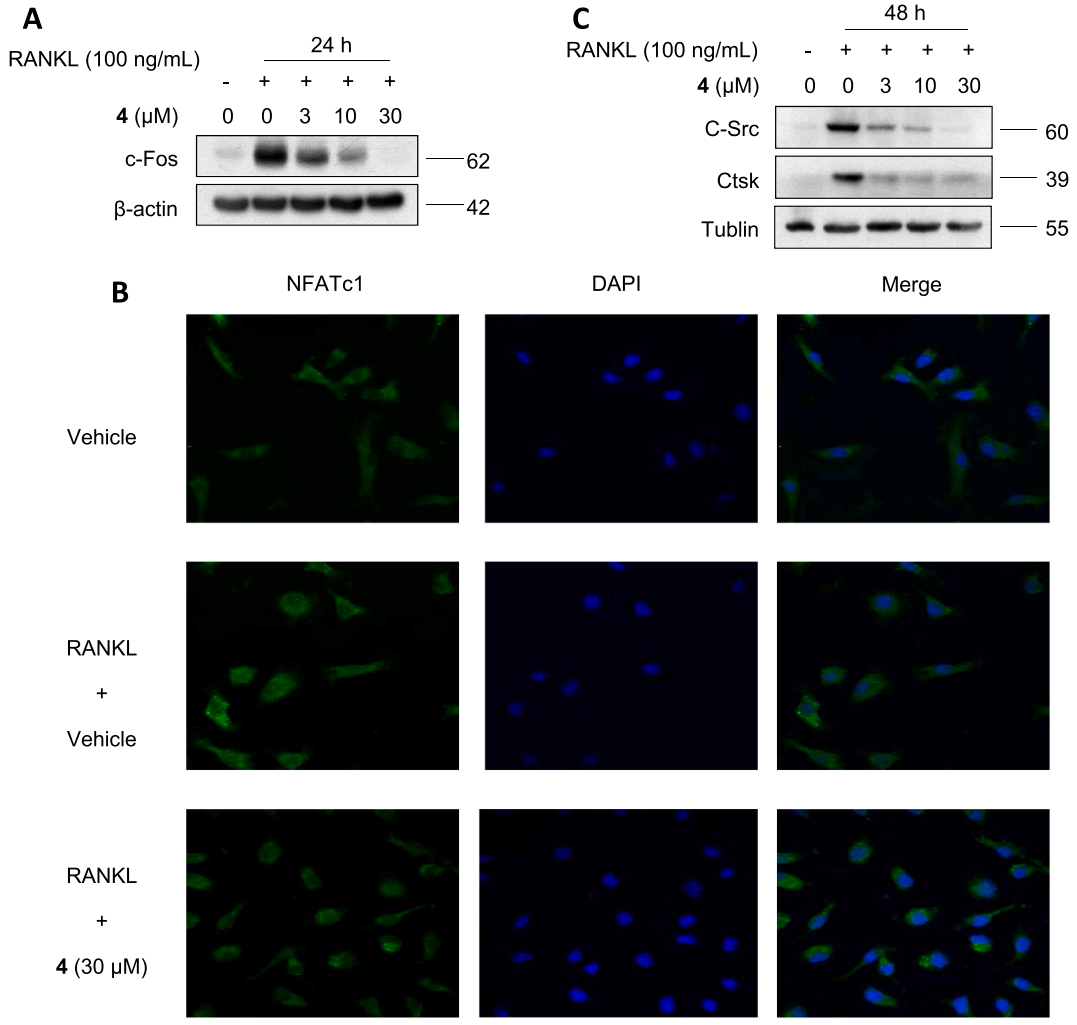

Fig. 5. Compound **4** inhibits RANKL-induced c-Fos and NFATc1 activation. (A) RAW264.7 cells were incubated with RANKL in the presence of indicated concentrations of compound **4**. The expression level of c-Fos was determined by Western blotting. (B) RAW264.7 cells were stimulated with RANKL for 48 h in the presence or absence of 30 μM compound **4**, and then fixed and stained with an anti-NFATc1 antibody, followed by an Alexa Fluor 488-conjugated secondary antibody. DAPI was used to stain nuclei. Scale bar: 10 μm. (C) RAW264.7 cells were stimulated with RANKL (100 ng/ml) in the presence of indicated concentrations of compound **4** for 48 h. The expression levels of CtsK and c-Src were determined by Western blotting.

with OCH_3 group at C-8, and showed the highest anti-osteoclastogenesis ability, while compounds **2** and **3** containing six OCH_3 groups, and exhibited weaker inhibition (Fig. 3). We later found that the OCH_3 group at C-8 appeared to enhance the inhibitory effect on osteoclast formation. Compound **3** showed higher activity than compound **2**, both having a similar number of OCH_3 groups except for the methoxyl group at C-8 in compound **3,** instead of at C-6 in compound **2**. Without OCH_3 at C-8, compounds **1** and **2** displayed similar inhibitory effect on RANKL-induced osteoclast differentiation. The above results indicate that the presence of the OCH_3 groups at the C-3, C-8 of the flavonoids played a crucial role in improving anti-osteoclastogenesis activity and that the number of OCH_3 groups in the structure of the flavonols promoted the inhibition of RANKL-induced osteoclast differentiation.

In conclusion, we described eight new flavonols (**7**–**9**, and **11**–**15**), together with sixteen known compounds (**1**–**6**, **10**, and **16**–**24**), all isolated from *C. unshiu* peels. Among them, compounds **1**–**4** inhibited RANKL-induced osteoclastogenesis in a dose-dependent manner. In addition, compound **4** inhibited actin-ring formation during the early stage of differentiation but had no cytotoxic effects. At the molecular level, compound **4** suppressed RANKL-induced c-Fos expression, and subsequently inhibited NFATc1 activation, as well as the expression of NFATc1 target genes, including CtsK and c-Scr, in a dose-dependent manner. These results suggest that compound **4** may potentially have a use as a therapeutic compound for the treatment or prevention of osteoclast-related diseases, such as osteoporosis.

Declaration of Competing Interest

The authors have no conflicts of interest to declare.

Acknowledgments

This research was supported by the National Research Foundation of Korea (NRF) funded by the Ministry of Science, ICT, and Future Planning (NRF-2018R1D1A1B07045287) and by the Korea government (MSIT) (No. NRF-2020R1A5A2017323). We are grateful to the Korea Basic Science Institute (KBSI) for mass spectrometric measurements.

Appendix A. Supplementary material

The supporting information including IR, UV, 1D and 2D NMR, HR-MS of compounds (**7**–**9**, and **11**–**15**), 1D NMR of known compounds (**1**–**6**, **16**–**24**), and anti-osteoclastogenesis effect of compounds **1**–**24** to this article can be found online. Supplementary data to this article can be found online at https://doi.org/10.1016/j.bioorg.2020.104613.

References

[1] J.T. Lin, J.M. Lane, Osteoporosis: A Review, Clin. Orthop. Relat. Res. 425 (2004) 126–134.
[2] L.J. Raggatt, N.C. Partridge, Cellular and molecular mechanisms of bone remodeling, J. Biol. Chem. 285 (33) (2010) 25103–25108, https://doi.org/10.1074/jbc.R109.041087.
[3] G.D. Roodman, Cell biology of the osteoclast, Exp. Hematol. 27 (8) (1999) 1229–1241, https://doi.org/10.1016/S0301-472X(99)00061-2.
[4] M. Asagiri, H. Takayanagi, The molecular understanding of osteoclast differentiation, Bone 40 (2) (2007) 251–264, https://doi.org/10.1016/j.bone.2006.09.023.
[5] D.B. Logar, R. Komadina, J. Preželj, B. Ostanek, Z. Trošt, J. Marc, Expression of bone resorption genes in osteoarthritis and in osteoporosis, J. Bone Miner. Metab. 25 (4) (2007) 219–225, https://doi.org/10.1007/s00774-007-0753-0.
[6] J.P. Bilezikian, L.G. Raisz, T.J. Martin, In Principles of Bone Biology, 4 th John Bilezikian, J., Martin, T. J, Clemens, T., Rosen, C., Elsevier, 2020, pp. 111–131.
[7] Y.-C. Oh, W.-K. Cho, Y.H. Jeong, G.Y. Im, M.C. Yang, Y.-H. Hwang, J.Y. Ma, Anti-Inflammatory Effect of *Citrus Unshiu* Peel in LPS-Stimulated RAW 264.7 Macrophage Cells, Am. J. Chin. Med. 40 (03) (2012) 611–629, https://doi.org/10.1142/S0192415X12500462.
[8] D.W. Lim, Y. Lee, Y.T. Kim, Preventive effects of *Citrus unshiu* peel extracts on bone and lipid metabolism in OVX rats, Molecules 19 (1) (2014) 783–794, https://doi.org/10.3390/molecules19010783.
[9] J.H. Lyu, H.-T. Lee, Effects of dried *Citrus unshiu* peels on gastrointestinal motility in rodents, Arch. Pharm. Res. 36 (5) (2013) 641–648, https://doi.org/10.1007/s12272-013-0080-z.
[10] Q.-M. Ngo, H.-S. Lee, V.T. Nguyen, J.A. Kim, M.H. Woo, B.S. Min, Chemical constituents from the fruits of *Ligustrum japonicum* and their inhibitory effects on T cell activation, Phytochemistry 141 (2017) 147–155, https://doi.org/10.1016/j.phytochem.2017.06.001.
[11] P.T. Tran, D.H. Park, O. Kim, S.H. Kwon, B.S. Min, J.H. Lee, Desoxyrhapontigenin inhibits RANKL-induced osteoclast formation and prevents inflammation-mediated bone loss, Int. J. Mol. Med. 42 (2018) 569–578, https://doi.org/10.3892/ijmm.2018.3627.
[12] P.T. Tran, T.-M. Ngo, S. Lee, O. Kim, H.N.K. Tran, C. Hwangbo, B.S. Min, J.-H. Lee, Identification of anti-osteoclastogenic compounds from *Cleistocalyx operculatus* flower buds and their effects on RANKL-induced osteoclastogenesis, J. Funct. Foods 60 (2019) 103388, https://doi.org/10.1016/j.jff.2019.05.044.
[13] T. Hòrie, Y. Ohtsuru, K. Shibata, K. Yamashita, M. Tsukayama, Y. Kawamura, ^{13}C NMR spectral assignment of the A-ring of polyoxygenated flavones, Phytochemistry 47 (5) (1998) 865–874, https://doi.org/10.1016/S0031-9422(97)00629-8.
[14] S. Li, C.-Y. Lo, C.-T. Ho, Hydroxylated Polymethoxyflavones and Methylated Flavonoids in Sweet Orange (Citrus sinensis) Peel, J. Agric. Food Chem. 54 (12) (2006) 4176–4185, https://doi.org/10.1021/jf060234n.
[15] D.K. Kim, K.T. Lee, J.S. Eun, O.P. Zee, J.P. Lim, S.S. Eum, S.H. Kim, T.Y. Shin, Anti-allergic components from the peels ofCitrus unshiu, Arch. Pharm. Res. 22 (6) (1999) 642–645, https://doi.org/10.1007/BF02975340.
[16] M.-A. Beck, H. Häberlein, Flavonol glycosides from *Eschscholtzia californica*, Phytochemistry 50 (2) (1999) 329–332, https://doi.org/10.1016/S0031-9422(98)00503-2.
[17] M.S. Hifnawy, A.MK. Mahrous, A.A. Sleem, R.MS. Ashour, Comparative chemical and biological studies of leaves and pollens of *Phoenix canariensis* hort. ex Chabaud, Future Med. Chem. 9 (9) (2017) 871–880, https://doi.org/10.4155/fmc-2017-0010.
[18] H.J. Eom, D. Lee, S. Lee, H.J. Noh, J.W. Hyun, P.H. Yi, K.S. Kang, K.H. Kim, Flavonoids and a Limonoid from the Fruits of *Citrus unshiu* and Their Biological Activity, J. Agric. Food Chem. 64 (38) (2016) 7171–7178, https://doi.org/10.1021/acs.jafc.6b03465.s001.
[19] H. Nagase, N. Omae, A. Omori, O. Nakagawasai, T. Tadano, A. Yokosuka, Y. Sashida, Y. Mimaki, T. Yamakuni, Y. Ohizumi, Nobiletin and its related flavonoids with CRE-dependent transcription-stimulating and neuritegenic activities, Biochem. Biophys. Res. Commun. 337 (4) (2005) 1330–1336, https://doi.org/10.1016/j.bbrc.2005.10.001.
[20] S.H. Lee, B.H. Moon, Y.H. Park, E.J. Lee, S. Hong, Y.H. Lim, Methyl substitution effects on ^{1}H and ^{13}C NMR data of methoxyflavone, Bull. Korean Chem. Soc. 29 (2008) 1793–1796.
[21] R.J. Ferracin, M.F. das G.F. da Silva, J.B. Fernandes, P.C. Vieira, Flavonoids from the fruits of *Murraya paniculata*, Phytochemistry 47 (3) (1998) 393–396, https://doi.org/10.1016/S0031-9422(97)00598-0.
[22] R.S. Compagnone, A.C. Suarez, S.G. Leitao, F. Delle Monache, Flavonoids, benzophenones and a new euphane derivative from *Clusia columnaris* Engl, Rev. Bras. Farmacogn. 18 (2008) 6–10.
[23] Y. Miyake, K. Yamamoto, Y. Morimitsu, T. Osawa, Isolation of *C*-glucosylflavone from lemon peel and antioxidative activity of flavonoid compounds in lemon fruit, J. Agric. Food Chem. 45 (12) (1997) 4619–4623, https://doi.org/10.1021/jf970498x.
[24] H. Nakagawa, Y. Takaishi, N. Tanaka, K. Tsuchiya, H. Shibata, T. Higuti, Chemical constituents from the peels of citrussudachi, J. Nat. Prod. 69 (8) (2006) 1177–1179, https://doi.org/10.1021/np060217s.s001.
[25] S.P.B. Ovenden, M. Cobbe, R. Kissell, G.W. Birrell, M. Chavchich, M.D. Edstein, Phenolic glycosides with antimalarial activity from *Grevillea* “Poorinda Queen”, J. Nat. Prod. 74 (1) (2011) 74–78, https://doi.org/10.1021/np100737q.
[26] N. Zhang, W.-X. Huang, G.-Y. Xia, M.B. Oppong, L.-Q. Ding, P. Li, F. Qiu, Methods for determination of absolute configuration of monosaccharides, Chinese Herbal Med. 10 (1) (2018) 14–22, https://doi.org/10.1016/j.chmed.2017.12.009.
[27] Y. Hattori, K.-H. Horikawa, H. Makabe, N. Hirai, M. Hirota, T. Kamo, A refined method for determining the absolute configuration of the 3-hydroxy-3-methylglutaryl group, Tetrahedron Asymmetry 18 (10) (2007) 1183–1186, https://doi.org/10.1016/j.tetasy.2007.05.013.
[28] S. Song, X. Zheng, W. Liu, R. Du, L. Bi, P. Zhang, 3-Hydroxymethylglutaryl flavonol glycosides from a mongolian and tibetan medicine, *Oxytropis racemosa*, Chem. Pharm. Bull. 58 (12) (2010) 1587–1590, https://doi.org/10.1248/cpb.58.1587.
[29] C. Li, Z. Yang, Z. Li, Y.u. Ma, L. Zhang, C. Zheng, W. Qiu, X. Wu, X. Wang, H. Li, J. Tang, M. Qian, D. Li, P. Wang, J. Luo, M. Liu, Maslinic acid suppresses osteoclastogenesis and prevents ovariectomy-induced bone loss by regulating RANKL-mediated NF-κB and MAPK signaling pathways, J Bone Miner Res 26 (3) (2011) 644–656, https://doi.org/10.1002/jbmr.242.
[30] J.H. Kim, N. Kim, Signaling pathways in osteoclast differentiation, Chonnam Med. J. 52 (1) (2016) 12–17, https://doi.org/10.4068/cmj.2016.52.1.12.
[31] Y.-Y. Choo, P.T. Tran, B.-S. Min, O. Kim, H.D. Nguyen, S.-H. Kwon, J.-H. Lee, Sappanone A inhibits RANKL-induced osteoclastogenesis in BMMs and prevents inflammation-mediated bone loss, Int. Immunopharmacol. 52 (2017) 230–237, https://doi.org/10.1016/j.intimp.2017.09.018.